Utility of MetaSite in Improving Metabolic Stability of the Neutral Indomethacin Amide Derivative and Selective Cyclooxygenase-2 Inhibitor 2-(1-(4-Chlorobenzoyl)-5-methoxy-2-methyl-1*H*-indol-3-yl)-*N*-phenethyl-acetamide

David Boyer, Jonathan N. Bauman, Daniel P. Walker, Brendon Kapinos, Kapil Karki, and Amit S. Kalgutkar

Pharmacokinetics, Dynamics and Metabolism Department and Discovery Chemistry, Pfizer Global Research and Development, Groton, Connecticut (D.B., J.N.B., B.K., K.K., A.S.K.); and Discovery Chemistry, Pfizer Global Research and Development, St. Louis Laboratories, Chesterfield, Missouri (D.P.W.)

ABSTRACT:

Prediction of the metabolic sites for new compounds, synthesized or virtual, is important in the rational design of compounds with increased resistance to metabolism. The aim of the present investigation was to use rational design together with MetaSite, an in silico tool for predicting metabolic soft spots, to synthesize compounds that retain their pharmacological effects but are metabolically more stable in the presence of cytochrome P450 (P450) enzymes. The model compound for these studies was the phenethyl amide (1) derivative of the nonsteroidal anti-inflammatory drug (NSAID) indomethacin. Unlike the parent NSAID, 1 is a potent and selective cyclooxygenase-2 (COX-2) inhibitor and nonulcerogenic anti-inflammatory agent in the rat. This pharmacological benefit is offset by the finding that 1 is very unstable in rat and human microsomes because of extensive P4503 A4/2D6-mediated metabolism on the phenethyl group, experimental observations that were accurately predicted by MetaSite. The information was used to design analogs with polar (glycinyl) and/or electron-deficient (fluorophenyl, fluoropyridinyl) amide substituents to reduce metabolism in 1. MetaSite correctly predicted the metabolic shift from oxidation on the amide substituent to *O*-demethylation for these compounds, whereas rat and human microsomal stability studies and pharmacokinetic assessments in the rat confirmed that the design tactics for improving pharmacokinetic attributes of 1 had worked in our favor. In addition, the fluorophenyl and pyridinyl amide derivatives retained the potent and selective COX-2 inhibition demonstrated with 1. Overall, the predictions from MetaSite gave useful information leading to the design of new compounds with improved metabolic properties.

In the early drug discovery phase, many compounds have high oxidative metabolic instability mediated by cytochrome P450 (P450) enzymes, which often results in poor oral pharmacokinetics in preclinical species. Whereas high-throughput in vitro microsomal assays that monitor metabolic stability provide a convenient means for "rank-ordering" large numbers of compounds, information pertaining to identification of "soft spots" for unstable compounds cannot be discerned from such analyses and requires separate metabolite identification studies. Unlike microsomal stability assays, metabolite identification experiments are low-throughput and cannot keep pace with high-speed chemistry efforts. In addition, there are scenarios in which metabolism studies will limit the labile site(s) to a certain region within the molecule. To guide chemists in the right direction, information on the exact metabolic site is often preferred. Therefore, in addition to existing in vitro assays, a value added proposition would

be the use of in silico tools to precisely predict regiochemistry of metabolism for compounds (synthesized or only virtual), information that could be used for rational design of pharmacologically active compounds with improved metabolic properties.

MetaSite is an in silico tool that can identify the most likely sites of P450-mediated oxidative metabolism in a compound (Cruciani et al., 2005) and has produced some success in de novo design of pharmacological compounds with improved metabolic properties (Ahlstrom et al., 2007). MetaSite is based on two factors: chemical reactivity of the substrate and enzyme-substrate similarity analysis. MetaSite performs a similarity analysis of the protein-cavity interaction profile and the potential substrate. The chemical reactivity of fragments toward oxidation, representing the activation energy of the conversion of substrate to metabolite, is precomputed and stored within the program. Consequently, if the similarity search gives a high score for a fragment, the chemical reactivity of that fragment is included in the final "hot spot" prediction (Zamora et al., 2003; Cruciani et al., 2005).

In this article, we have explored the performance of MetaSite as a

---

ABBREVIATIONS: P450, cytochrome P450; COX, cyclooxygenase; NSAID, nonsteroidal anti-inflammatory drug; DMSO, dimethyl sulfoxide; MS, mass spectrometry; ESI, electrospray ionization; LC, liquid chromatography; MS/MS, tandem mass spectrometry; MRM, multiple reaction monitoring; CID, collision-induced dissociation; AUC, area under the plasma concentration-time curve.
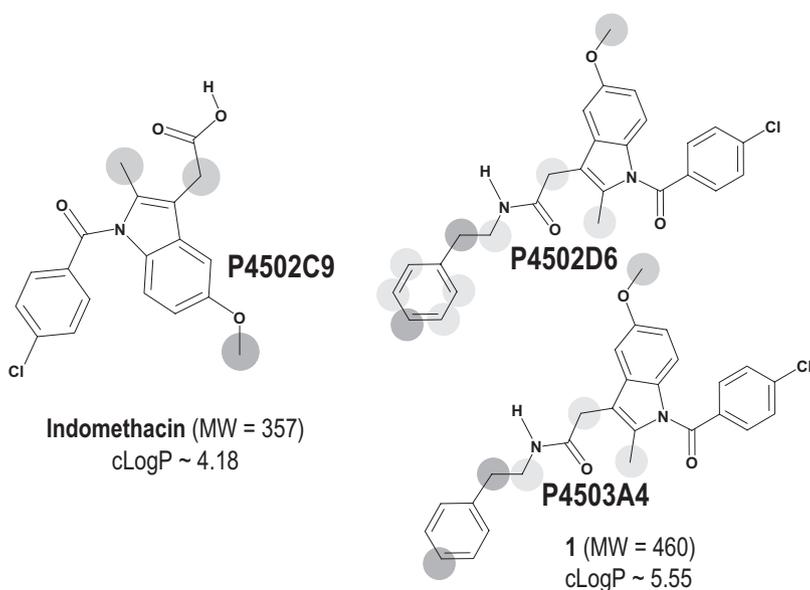
FIG. 1. Plots of MetaSite predictions for sites of metabolism for indomethacin and 2-(1-(4-chlorobenzoyl)-5-methoxy-2-methyl-1*H*-indol-3-yl)-*N*-phenethyl-acetamide (**1**). The functional groups in both compounds that most likely will be metabolized are marked: the darker the color the higher the probability of metabolism to occur. Because oxidative metabolism (*O*-demethylation) of indomethacin is exclusively by P450 2C9 (Nakajima et al., 1998), in silico predictions were only made with P450 2C9. Likewise, because P450 3A4 and P450 2D6 are involved in the metabolism of **1**, we chose the software's ability to predict contributions from these two P450 isozymes. MW, molecular weight.

tool to guide drug discovery efforts when prior information on metabolic fate does not exist. For this endeavor, we chose a series of selective cyclooxygenase (COX)-2 inhibitors comprising neutral amide derivatives of the nonsteroidal anti-inflammatory drug (NSAID) indomethacin as target compounds for optimization (Fig. 1) (Kalgutkar et al., 2000a,b). Indomethacin is a nonselective inhibitor of the COX isozymes, COX-1 and COX-2, but derivatization of its carboxylic acid group to ester or amide analogs produces compounds that are highly selective and potent COX-2 inhibitors. 2-(1-(4-Chlorobenzoyl)-5-methoxy-2-methyl-1*H*-indol-3-yl)-*N*-phenethyl-acetamide (**1**) (Fig. 1) is a prototypical compound (>1000-fold COX-2 selectivity) in the series that demonstrates in vivo anti-inflammatory activity comparable with that of indomethacin but is devoid of the ulcerogenic effects associated with the parent NSAID (Kalgutkar et al., 2000a). The attractive pharmacological and safety advantage of **1** over indomethacin, however, is offset by the metabolic instability of **1** in rat and human liver microsomes ($t_{1/2}$ <5 min) compared with that of indomethacin ($t_{1/2}$ >60 min) (Remmel et al., 2004; Obach et al., 2008). Consistent with the in vitro finding, **1** exhibited a very short $t_{1/2}$ (<20 min) upon intravenous administration to rats (Remmel et al., 2004). In vitro metabolism studies in human liver microsomes identified oxidations on the pendant phenethyl substituent by P450 3A4 and *O*-demethylation by P450 2D6 as the principal metabolic routes (Remmel et al., 2004).

In the first set of experiments, we used MetaSite retrospectively to predict P450-derived metabolites of **1** and indomethacin (for comparative purposes). Predictions were then compared with experimental data. Next, we applied MetaSite to predict metabolites for virtual indomethacin amides (Fig. 2) for which no prior knowledge on their metabolic fate existed. In this exercise, appropriate structural modifications were included in the virtual structures to reduce P450 metabolism. The virtual compounds were synthesized, and experimental in vitro metabolism data (compound stability, metabolite identification, and P450 phenotyping) were generated for the analogs. The synthesized compounds along with **1** were administered to rats to examine whether the structural changes afforded overall improvements in clearance. The collective findings of these analyses are summarized herein.

Materials and Methods

Materials. Unless stated otherwise, all chemicals, reagents, and solvents used in organic synthesis were purchased from Sigma-Aldrich (St. Louis, MO) and were used without any further purification. Fluoro-pyridin-3-amine was purchased from Matrix Scientific (Columbia, SC). ^{1}H NMR spectra were recorded on a Varian INOVA 400 MHz spectrometer. Chemical shifts are reported in parts per million (δ) relative DMSO-d₆ (δ 2.50). Spin multiplicities are given as s (singlet), d (doublet), dd (doublet of doublets), t (triplet), and m (multiplet). Low-resolution mass spectra were obtained on a 1946C Agilent MSD single quad mass spectrometer (Agilent Technologies, Santa Clara, CA) operating in a positive electrospray mode. Reactions were monitored by thin-layer chromatography using precoated silica gel GHLF plates (0.25-mm thickness) (Analtech, Newark, DE). The plates were visualized by a UV lamp. 2-(1-(4-Chlorobenzoyl-5-methoxy-2-methyl-1*H*-indo-3-yl)-*N*-(phenethyl)-acetamide (**1**) was synthesized as described previously (Kalgutkar et al., 2000b). Pooled human and rat liver microsomes and recombinant P450 isozymes were purchased from BD Gentest (Woburn, MA). Reduced NADPH, ketoconazole, and quinidine were purchased from Sigma-Aldrich.

2-(1-(4-Chlorobenzoyl)-5-methoxy-2-methyl-1*H*-indol-3-yl)-*N*-(4-fluorophenyl)acetamide (2). To a stirred solution of indomethacin (1.6 g, 4.5 mmol) in methylene chloride (20 ml) at room temperature were added oxalyl chloride (0.42 ml, 4.9 mmol) and anhydrous dimethylformamide (35 μl, 0.45 mmol). The mixture was stirred for 2 h at room temperature. 4-Fluoroaniline (990 mg, 9.0 mmol) was then added, and the mixture was stirred overnight at room temperature. The reaction mixture was diluted with water and methylene chloride. The organic layer was washed successively with 1.0 M aqueous hydrochloric acid solution, 1.0 M aqueous sodium hydroxide solution, and brine. The organic layer was dried over anhydrous magnesium sulfate, filtered, and concentrated in vacuo. The residue was triturated in *tert*-butyl methyl ether, which caused a white precipitate to form. The precipitate was filtered and washed with *tert*-butyl methyl ether. The precipitate was dried in vacuo to afford 1.4 g (70%) of **2** as a white solid. ^{1}H NMR (DMSO-d₆) δ 10.23 (br s, 1H), 7.65 (d, 2H, *J* = 8.0 Hz), 7.61 (d, 2H, *J* = 8.0 Hz), 7.58 (dd, 2H, *J* = 8.0, 4.0 Hz), 7.14 (d, 1H, *J* = 4.0 Hz), 7.10 (t, 2H, *J* = 8.0 Hz), 6.89 (d, 1H, *J* = 8.0 Hz), 6.68 (dd, 1H, *J* = 8.0, 4.0 Hz), 3.71 (s, 3H), 3.70 (s, 2H), 2.24 (2, 3H); low resolution MS (ESI) *m/z* 450.9 [M + H].

2-(1-(4-Chlorobenzoyl)-5-methoxy-2-methyl-1*H*-indol-3-yl)-*N*-(6-fluoropyridin-3-yl)acetamide (3). This compound was prepared from indomethacin (1.6 g, 4.5 mmol) and 6-fluoropyridin-3-amine (1.0 g, 9.0 mmol) in a manner similar to that described for compound **2** in 60% yield (1.2 g). The title compound was isolated as a white solid. ^{1}H NMR (DMSO-d₆) δ 10.48 (br s, 1H), 8.40 (m, 1H), 8.13 (m, 1H), 7.67 (d, 2H, *J* = 8.0 Hz), 7.62 (d, 2H, *J* = 8.0 Hz), 7.14 (d, 1H, *J* = 4.0 Hz), 7.12 (dd, 1H, *J* = 8.0, 4.0 Hz), 6.91 (d, 1H,
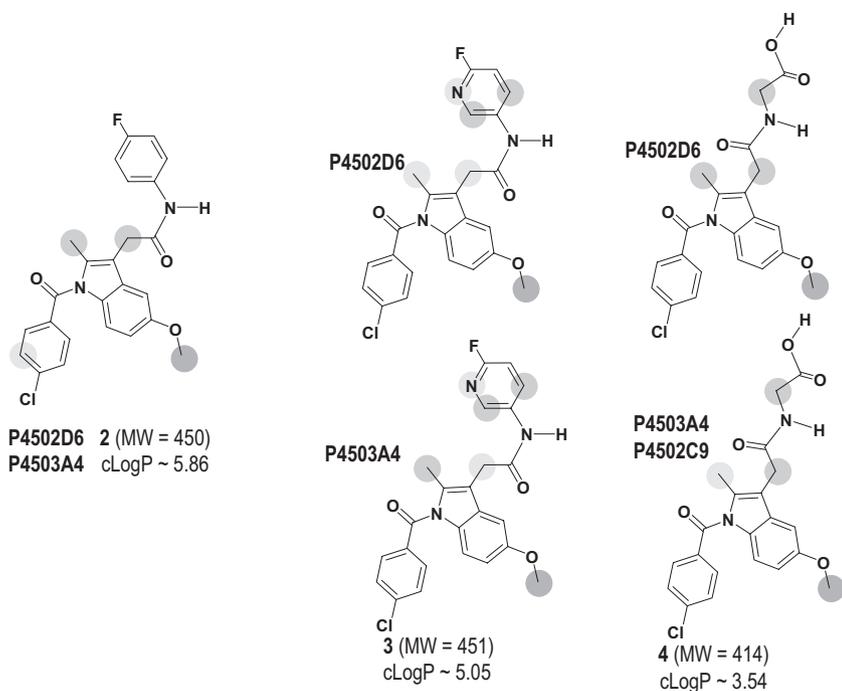
FIG. 2. Plots of MetaSite predictions for sites of metabolism of neutral indomethacin amide derivatives. The functional groups in both compounds that most likely will be metabolized are marked: the darker the color the higher the probability of metabolism to occur. Based on the available P450 phenotyping information for **1**, we chose the software's ability to predict metabolism by P450 3A4 and P450 2D6 for compounds **2** and **3** and by P450 3A4, 2D6, and 2C9 for compound **4**. This in silico data were generated in a virtual fashion (i.e., before the actual synthesis of the compounds). MW, molecular weight.

J = 8.0 Hz), 6.69 (dd, 1H, J = 8.0, 4.0 Hz), 3.76 (s, 2H), 3.72 (s, 3H), 2.25 (s, 3H); low resolution MS (ESI) *m/z* 451.9 [M + H].

2-(2-(1-(4-Chlorobenzoyl)-5-methoxy-2-methyl-1*H*-indol-3-yl)acetamido)-acetic acid (4). *Step 1: Preparation of tert-butyl-2-(2-(1-(4-chlorobenzoyl)-5-methoxy-2-methyl-1H-indol-3-yl)acetamido)acetic acetate.* The *tert*-butylglycine amide derivative was synthesized from indomethacin (1.6 g, 4.5 mmol) and glycine *tert*-butyl ester (1.2 g, 9.0 mmol) via a procedure similar to that described for **2**. The compound was isolated as a white solid in 90% yield (1.9 g). ^{1}H NMR (DMSO-d$_6$) δ 8.24 (t, 1H, J = 4.0 Hz), 7.65 (d, 2H, J = 8.0 Hz), 7.59 (d, 2H, J = 8.0 Hz), 7.08 (d, 1H, *J* 4.0 Hz), 6.90 (d, 1H, J = 8.0 Hz), 6.65 (dd, 1H, J = 8.0, 4.0 Hz), 3.72 (s, 3H), 3.67 (d, 2H, J = 4.0 Hz), 3.53 (s, 2H), 2.18 (s, 3H), 1.33 (s, 9H); low resolution MS (ESI) *m/z* 492.9 [M + Na].

Step 2. To a stirred solution of indomethacin-*tert*-butylglycine amide (1.0 g, 2.1 mmol) in methylene chloride (20 ml) was added trifluoroacetic acid (10 ml). The solution was stirred at room temperature for 1 h and then concentrated in vacuo. The remaining yellow residue was triturated in *tert*-butyl methyl ether to give a white precipitate. The precipitate was filtered and washed with *tert*-butyl methyl ether. The precipitate was dried in vacuo to afford 0.75 g (85%) of **4** as a white solid. ^{1}H NMR (DMSO-d$_6$) δ 12.50 (br s, 1H), 8.25 (t, 1H, J = 4.0 Hz), 7.64 (d, 2H, J = 8.0 Hz), 7.59 (d, 2H, J = 8.0 Hz), 7.09 (d, 1H, J = 4.0 Hz), 6.90 (d, 1H, J = 8.0 Hz,), 6.65 (dd, 1H, J = 8.0, 4.0 Hz), 3.72 (s, 3H), 3.71 (d, 2H, J = 4.0 Hz), 3.52 (s, 2H), 2.17 (s, 3H); low resolution MS (ESI) *m/z* 414.9 [M + H].

Modeling of Metabolism of Indomethacin and Its Analogs. All calculations were performed on a Windows Pentium personal computer. The software used in the computational analysis was MetaSite (version 2.8.7; Molecular Discovery Ltd., http://moldiscovery.com). Two-dimensional structures of the compounds (generated in a simplified molecular input line entry system notation) were submitted to the MetaSite program, which is a fully automated procedure. The MetaSite version used in this analysis contains the homology three-dimensional models of P450 1A2, P450 2C9, P450 2C19, P450 2D6, and P450 3A4 (Cruciani et al., 2005). MetaSite analyses to predict sites of metabolism involve the calculation of two sets of descriptors: one set for P450 enzyme(s) and one set for substrate. The resulting analysis provides a "chemical fingerprint" of the enzyme and the substrate. Chemical fingerprints are distance-based descriptors that are calculated from molecular interaction forces computed by GRID. MetaSite considers the chemical reactivity of the compound by taking into consideration the activation energy in the hydrogen abstraction step that ultimately generates metabolite(s). Hydrogen abstraction processes have been simulated by ab initio calculations of small fragments from drug-like substrates for human P450s and stored in MetaSite. When a fragment in

the target molecule is recognized as one in the MetaSite database, all atoms in that fragment are assigned the corresponding reactivity value. The final ranking for potential metabolic sites is the product of the similarity analysis and the chemical reactivity. Once the structures of the compounds are provided, the semiempirical calculations, pharmacophore recognition, descriptor handling, similarity, and reactivity computation are all performed automatically.

Incubations with Liver Microsomes. *Microsomal stability.* Stock solutions of test substrates were prepared in methanol. The final concentration of methanol in the incubation media was 0.2% (v/v). $t_{1/2}$ assessments in microsomes were determined in duplicate after incubation of test substrates (1 μM) with rat or human liver microsomes (P450 concentration, 0.25 μM) in 0.1 M potassium phosphate buffer (pH 7.4) at 37°C. The total incubation volume was 0.6 ml. The reaction mixture was prewarmed at 37°C for 2 min before addition of NADPH (1.2 mM). Aliquots (75 μl) of the reaction mixture at 0, 5, 15, and 30 min (time period associated with reaction linearity) were added to acetonitrile (200 μl) containing diclofenac (0.05 μg/ml) as internal standard, and the samples were centrifuged at 2500*g* for 5 min before liquid chromatography (LC)-tandem mass spectrometry (MS/MS) analysis of substrate disappearance. For control experiments, NADPH and or liver microsomes were omitted from these incubations. To assess the involvement of P450 3A4 and P450 2D6 isoforms in the metabolism of indomethacin amide derivatives, separate incubations were conducted wherein the P450 3A4-specific inhibitor ketoconazole (1 μM) or the P450 2D6 inhibitor quinidine (3 μM) was added to human liver microsomal incubations containing test substrate and NADPH, and the stability was reassessed in the presence of inhibitor.

Metabolite identification. For the purposes of metabolite identification studies, the concentration of test compound in the microsomal incubations was raised to 20 μM and that of P450 in rat and human liver microsomes was raised to 0.5 μM. The duration of the incubation time was increased from 30 to 45 min. After quenching the incubation mixtures with 2 volumes of acetonitrile, the solutions were centrifuged (3000*g*, 15 min), and the supernatants were dried under a steady nitrogen stream. The residue was reconstituted with the mobile phase and analyzed for metabolite formation by LC-MS/MS.

In Vivo Studies. Animal care and in vivo procedures were conducted according to guidelines of the Pfizer Animal Care and Use Committee. Jugular vein-cannulated male Sprague-Dawley rats (230–250 g), obtained from Charles River Laboratories (Wilmington, MA), were used for these studies. All animals were housed individually. All animals were fasted overnight before dosing, whereas access to water was provided ad libitum. Animals were fed after collection of the 4-h blood samples. Test compounds **1** to **4** were administered intravenously via the jugular vein of rats over 30 s at 1.0 mg/kg,
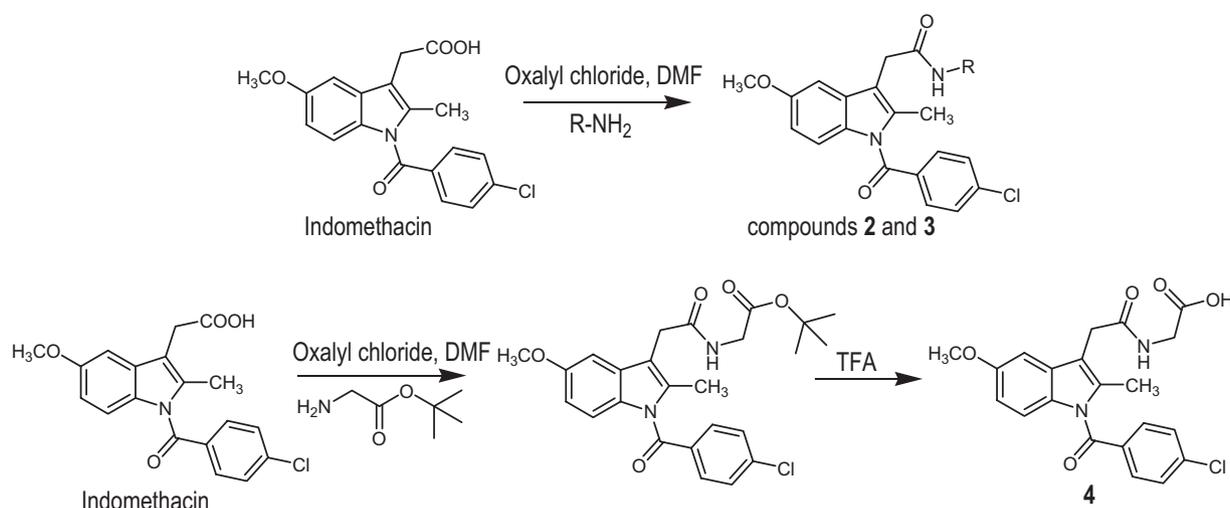
FIG. 3. Chemical preparation of the indomethacin amides used in the studies. DMF, dimethylformamide; TFA, trifluoroacetic acid.

respectively, and serial blood samples were collected before dosing and at 0.083, 0.15, 0.5, 1, 2, 4, 6, 8, and 24 h after dosing. The vehicle used in intravenous administration was 95% glycerol formal containing 5% DMSO. Test compounds **1** to **4** were also administered orally at 5.0 mg/kg as solutions in polyethylene glycol 400. Blood samples were taken before oral administration, and then serial samples were collected at 0.15, 0.5, 1, 2, 4, 6, 8, and 24 h after dosing. Blood samples from the various pharmacokinetic studies were centrifuged at 3000 rpm for 10 min at 4°C to generate plasma. All plasma samples were kept frozen until analysis. Aliquots of plasma (100 μl) were transferred to 96-well blocks, and acetonitrile (200 μl) containing diclofenac as internal standard (50 ng/ml) was added to each well. Samples were prepared for analysis by solid-phase extraction using a Waters Oasis MAX (10 mg) extraction plate (Waters, Milford, MA), following the manufacturer's directions. After extraction, the samples were then analyzed by LC-MS/MS, and concentrations of analyte in plasma were determined by interpolation from a standard curve.

Metabolite Identification Using Triple Quadrupole Linear Ion Trap LC-MS/MS. The LC system consisted of LC20AD pumps, a DGU20A5 degasser, and a VP Option box (Shimadzu, Columbia, MD), an HTC PAL autosampler (Leap Technologies, Cary, NC), and a Luna C8(2) (4.6 × 150 mm, 4 μm) high-performance liquid chromatography column (Phenomenex, Torrance, CA). LC mobile phase A was formic acid in water (0.1% v/v), and mobile phase B was formic acid in acetonitrile (0.1%). The flow rate was 0.7 ml/min. The LC gradient started at 5% B for 5 min, ramped linearly to 90% B over 30 min, held at 90% B over 5 min, and then returned to the initial condition over 1.0 min. Postcolumn flow was split such that the mobile phase was introduced into the mass spectrometer via an electrospray interface at a rate of 175 μl/min. The remaining flow was diverted to the photodiode array detector to provide simultaneous UV detection (λ = 254 nm) and a total ion chromatogram. The LC system was interfaced to an API 4000 Q-trap mass spectrometer (MDS Sciex, Toronto, ON, Canada) equipped with a TurboIon-Spray source. Metabolites were characterized in the full scan mode (from m/z 100 to 850) by the multiple reaction monitoring (MRM)-enhanced product ion mode after preset MRM transitions derived from the collision-induced dissociation (CID) information and using precursor ion scans with the major common fragment ion, m/z 139. Structural information was generated from the CID spectra of the corresponding protonated molecular ions.

Analytical Methodology for Indomethacin Amides. Substrate depletion in liver microsomal incubations and analyte concentrations in plasma samples were monitored on a Sciex API model 3000 LC/MS/MS system triple quadrupole mass spectrometer. Analytes were chromatographically separated using a Hewlett Packard series 1100 high-performance liquid chromatography system. An autosampler was programmed to inject 20 μl on a PrimeSphere 5 μ C18-HC 30 × 2.0 mm column (Phenomenex) using a mobile phase consisting of 10 mM ammonium acetate buffer-acetonitrile (60:40 v/v) containing 0.2%

(v/v) triethylamine and 0.1% (v/v) acetic acid at a flow rate varying from 1 to 1.5 ml/min. Ionization was conducted in the positive ion mode at the ionspray interface temperature of 400°C, using nitrogen for the nebulizing and heating gas. The ion spray voltage was 5.0 kV, and the orifice voltage was optimized at 30 eV. Substrates and internal standard were analyzed in the MRM mode. For test compounds, diagnostic transitions were obtained via separate studies involving direct infusion of the compounds into the mass spectrometer. For $t_{1/2}$ determinations in substrate depletion experiments in liver microsomes, substrate/internal standard peak height ratios were determined and normalized to the value obtained at time $t = 0$. The percentage of substrate remaining versus time was fitted to first-order decay functions to yield in vitro $t_{1/2}$ values. If the test substrate demonstrated nonlinearity on log percentage remaining versus time curves, only those initial time points wherein log-linearity was observed were used to determine $t_{1/2}$ values. For plasma samples from pharmacokinetic studies, calibration curves were prepared by plotting the appropriate peak area ratios against the concentrations of analyte in plasma using $1/x$ weighting of analyte/internal standard peak height ratios. The concentration of the analytes in the plasma samples was determined by interpolation from the standard curve. The dynamic range of the assay was 5 to 2500 ng/ml.

Pharmacokinetic Data Analysis. Plasma concentration-time profiles were analyzed using the well established noncompartmental method in WinNonlin (version 2.1; Pharsight, Mountain View, CA). Plasma clearance (CL_p) was calculated as the intravenous dose divided by the plasma concentration-time curve (AUC) from zero to infinity ($AUC_{0-\infty}$). $AUC_{0-\infty}$ was calculated by the linear trapezoid rule. The terminal slope of the ln(concentration) versus time plot was calculated by linear least-squares regression and the half-life was calculated as 0.693 divided by the absolute value of the slope. The steady-state volume of distribution (V_{dss}) was determined using noncompartmental analysis as follows:

$$V_{dss} = (\text{i.v. dose} \times \text{AUMC})/(\text{AUC})^2$$

where AUMC is the total area under the first moment of the drug concentration-time curve from time 0 to infinity. The relative bioavailability (F) of the oral doses was calculated by using the following equation:

$$F = \text{AUC}_{0-\infty}^{\text{p.o.}}/\text{AUC}_{0-\infty}^{\text{i.v.}} \times \text{dose}^{\text{i.v.}}/\text{dose}^{\text{p.o.}}$$

Results

Chemistry. As depicted in Fig. 3, well established methodology was used in the synthesis of the amide derivatives of indomethacin. Indomethacin amides **1** to **3** were prepared by treatment with the appropriate amine (or hydroxyl amine) derivatives using oxalyl chloride as the carboxylic acid activator. Indomethacin glycine analog **4** was synthesized in two steps via initial coupling of indomethacin with *tert*-butylglycine ester in the presence of oxalyl chloride followed by
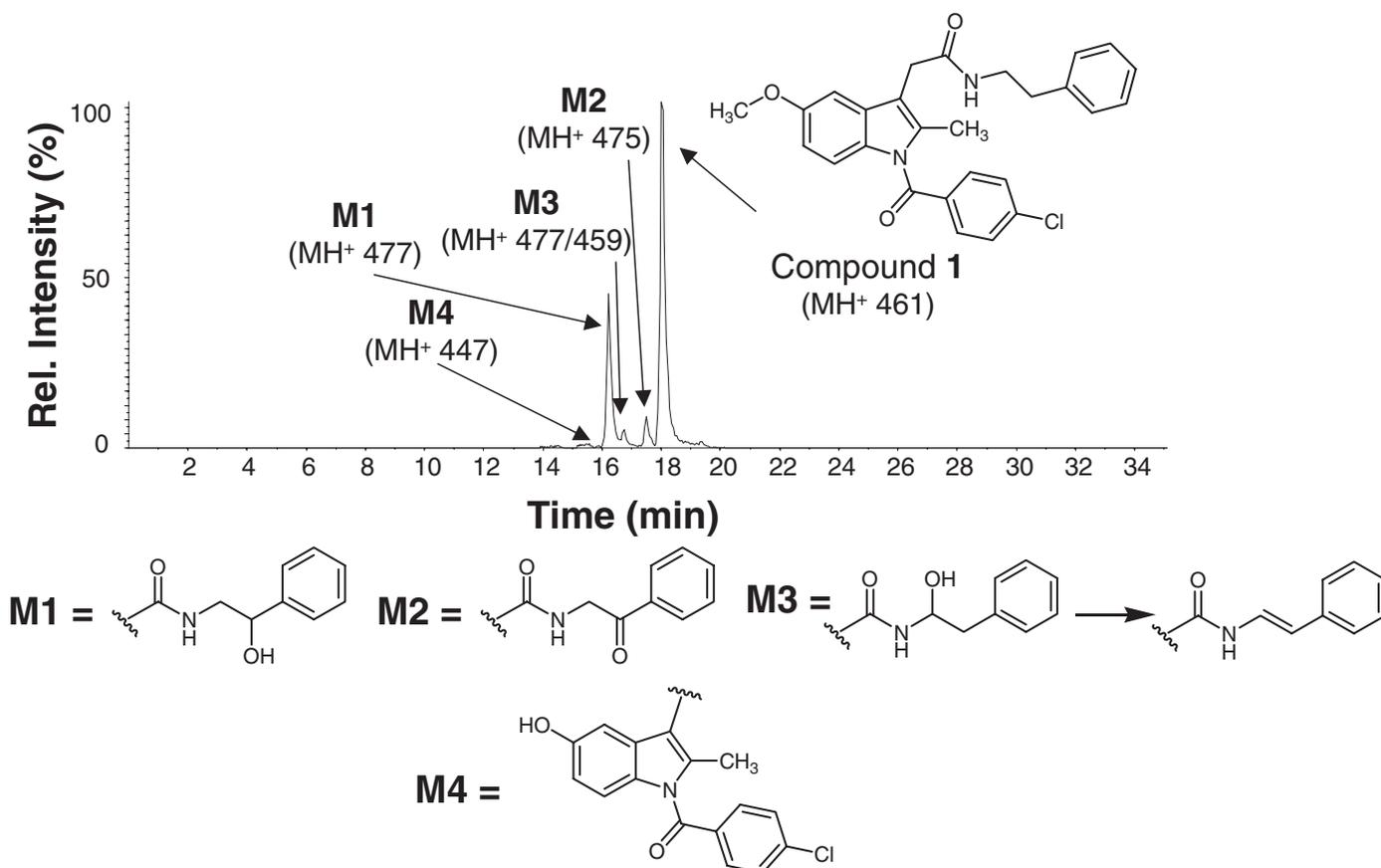
FIG. 4. LC-MS/MS analysis of an incubation mixture containing indomethacin-*N*-phenethyl amide (**1**) (20 μM) and NADPH-supplemented human liver microsomes. The structures of metabolites **M1** to **M4** are also depicted; these metabolites were also observed by Remmel et al. (2004) in an independent metabolism study on **1**.

acid-catalyzed ester hydrolysis of the intermediate indomethacin-*tert*-butylglycine amide.

Prediction of the Metabolic Fate of Indomethacin and Indomethacin-*N*-phenethyl Amide (1) by MetaSite. The P450 2C9 homology model in the software was used to predict indomethacin metabolites because the isozyme is principally responsible for oxidative metabolism of the NSAID (Nakajima et al., 1998). Metabolism prediction for **1** was restricted to P450 3A4/P450 2D6, given the role these isoforms play in the biotransformation of **1** (Remmel et al., 2004). The predictions for both compounds were executed without any input of information of known metabolites. As shown in Fig. 1, MetaSite correctly predicted the P450 2C9-catalyzed *O*-demethylation of indomethacin as the most likely biotransformation pathway. In the case of **1**, MetaSite predicted that P450 3A4- and P4502D6-mediated oxidations would occur principally on the phenethyl substituent (benzylic CH$_2$ and *para*-position on the phenyl ring); next in hierarchy was the prediction of *O*-demethylation by the two isozymes (Fig. 1). MetaSite prediction of benzylic oxidation by P4503A4 as the most plausible metabolic fate proved to be accurate because the principal metabolic fate of **1** in NADPH-supplemented human liver microsomes has been unambiguously shown to involve mono-hydroxylation on the benzylic carbon (metabolite **M1**) followed by further oxidation of this secondary alcohol metabolite to the ketone derivative **M2**. In addition to benzylic oxidation, MetaSite predicted *para*-aromatic hydroxylation on the phenethyl substituent as a very likely pathway. This prediction was incorrect because Remmel et al. (2004) have proven (using a synthetic standard of *para*-hydroxy-**1**) that **1** is not prone to aromatic ring hydroxylation. MetaSite predicted

that the possibility of oxidation on the carbon α to the amide nitrogen yielding **M3** and *O*-demethylation to **M4** was low, and indeed this turned out to be the case. Interestingly, MetaSite indicated that *O*-demethylation in **1** to metabolite **M4** was likely to be catalyzed by both P450 3A4 and P450 2D6, but in reality this metabolic sequence occurs only via P450 2D6 (Remmel et al., 2004). The metabolic profile of **1** in human liver microsomes is shown in Fig. 4 and is similar to that observed by Remmel et al. (2004).

Prediction of the Metabolic Fate of Novel Indomethacin Amide Derivatives by MetaSite. Considering that the *N*-linked substituent in **1** is the most prone to oxidative metabolism by P4503A4, we designed virtual compounds **2** to **4**, in which we introduced electron-deficient (e.g., *N*-fluorophenyl and *N*-fluoropyridinyl) or polar (glycine derivative **4**) *N*-substituents to reduce oxidative metabolic liability in this region. For the anilide analogs **2** and **3**, the electron-deficient fluorophenyl and fluoropyridinyl ring systems were also chosen to avoid reactive metabolite formation via aromatic hydroxylation *para* to the acetanilide nitrogen followed by two-electron oxidation to the electrophilic quinone-imine in a manner similar to that observed with acetaminophen (Dahlin et al., 1984). Upon presentation of compounds **2** to **4** to MetaSite, the prediction in each case shifted from metabolism on the *N*-substituent to *O*-demethylation as the most likely route of metabolism mediated by P450 3A4 and P450 2D6 for compounds **2** and **3** and by P450 enzymes 3A4, 2D6, and 2C9 for carboxylic acid derivative **4** (Fig. 2). Indeed, this was a fairly precise prediction because upon synthesis of **2** to **4** and testing for metabolism in NADPH-supplemented human liver microsomes, *O*-demethylation was observed as an almost exclusive pathway for the three compounds
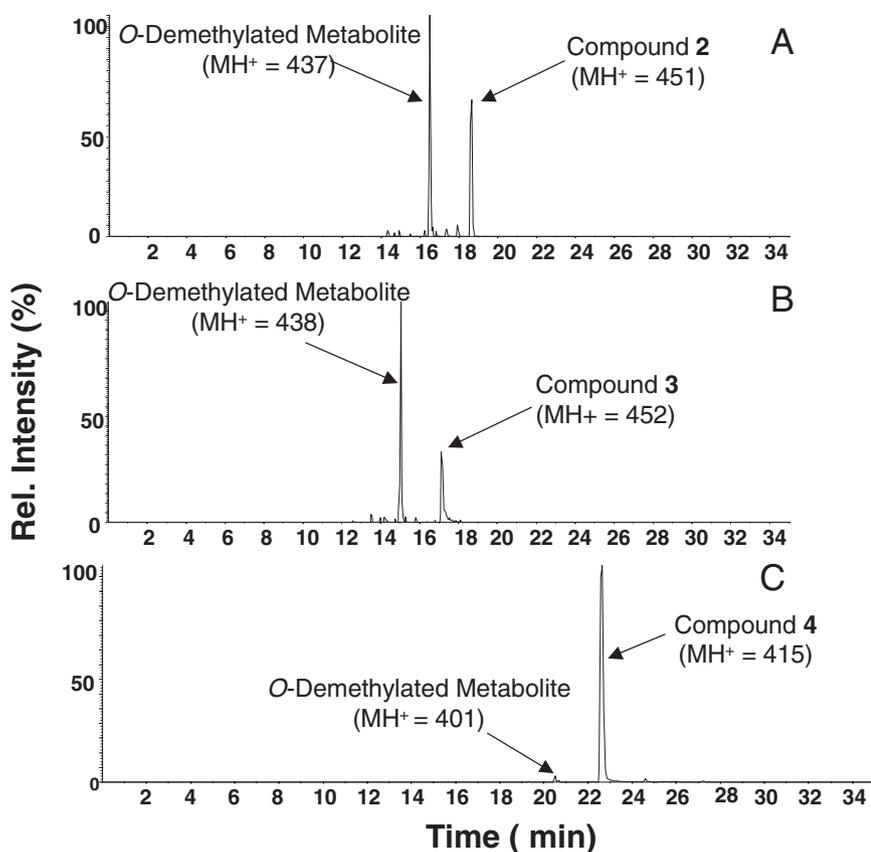
FIG. 5. LC-MS/MS analysis of an incubation mixture containing indomethacin-4-fluorophenyl amide (**2**) (A), indomethacin-4-fluoropyridinyl amide (**3**) (B), and indomethacin-glycine amide (**4**) (C) (20 μM concentrations each) and NADPH-supplemented human liver microsomes.

(Figs. 5–8). As for **1** (Remmel et al., 2004), indomethacin, a potential metabolite arising from amidase-mediated hydrolysis of compounds **2** to **4**, was not observed in these incubations.

Liver Microsomal Stability Assessments for Indomethacin Amide Derivatives and Identification of P450 Isozymes Responsible for Metabolism. The microsomal stability of indomethacin and
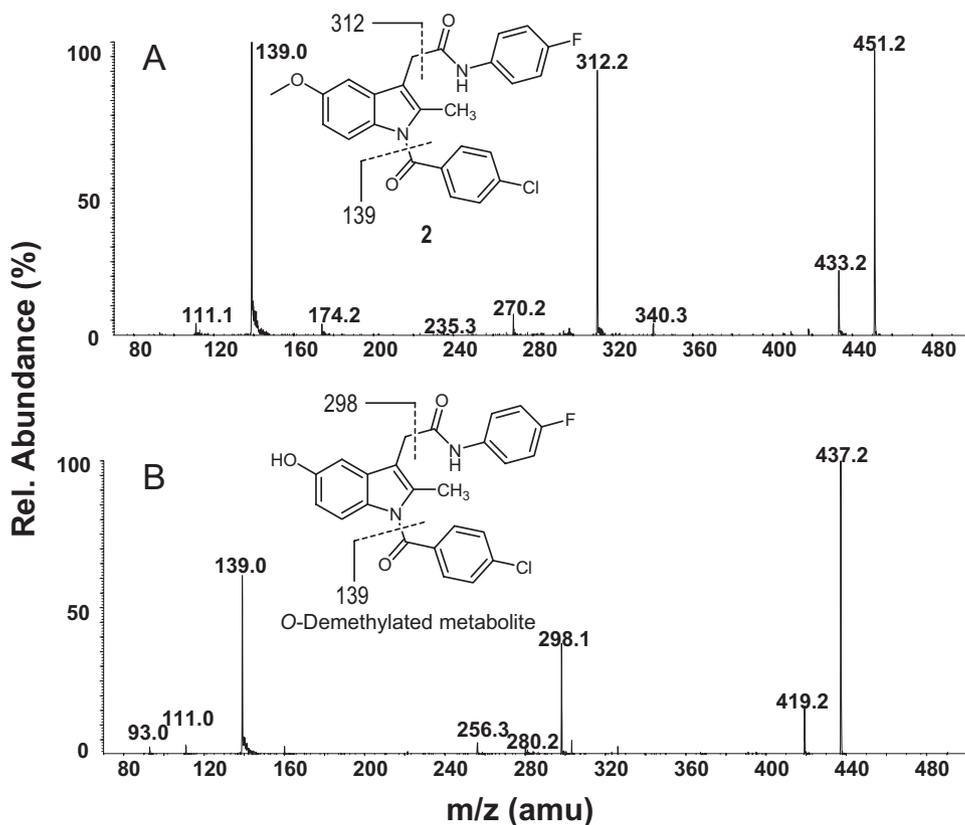

FIG. 6. CID spectrum of indomethacin-4-fluorophenyl amide (**2**) (A) and its *O*-demethylated metabolite (B). amu, atomic mass units.
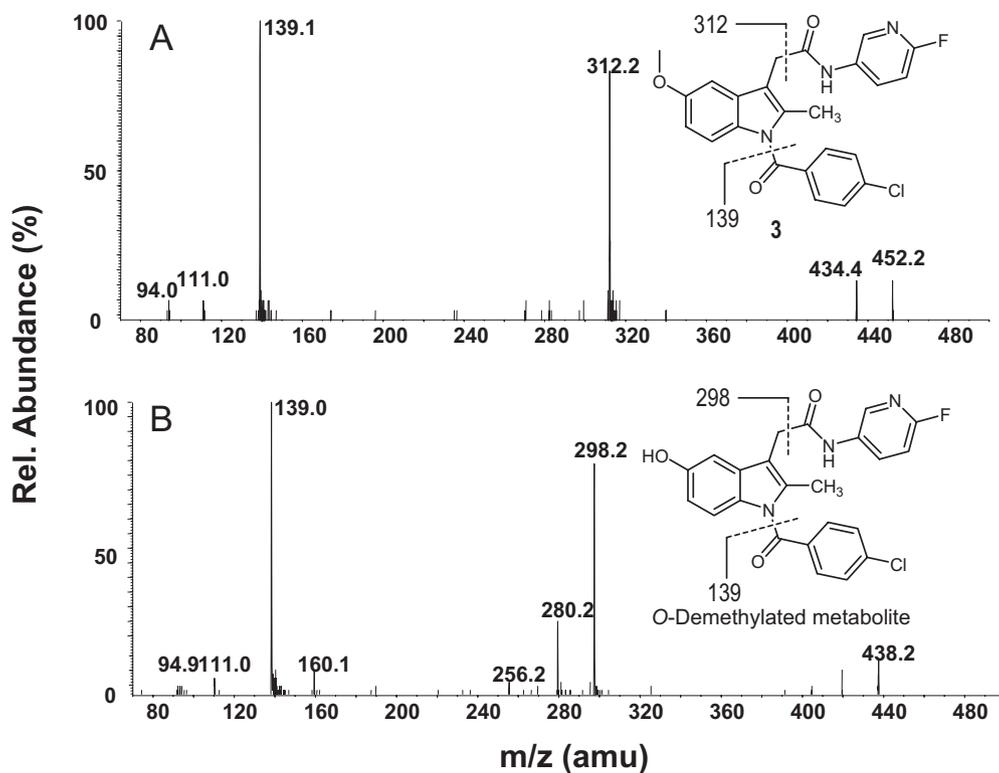
FIG. 7. CID spectrum of indomethacin-4-fluoropyridinyl amide (**3**) (A) and its *O*-demethylated metabolite (B). amu, atomic mass units.
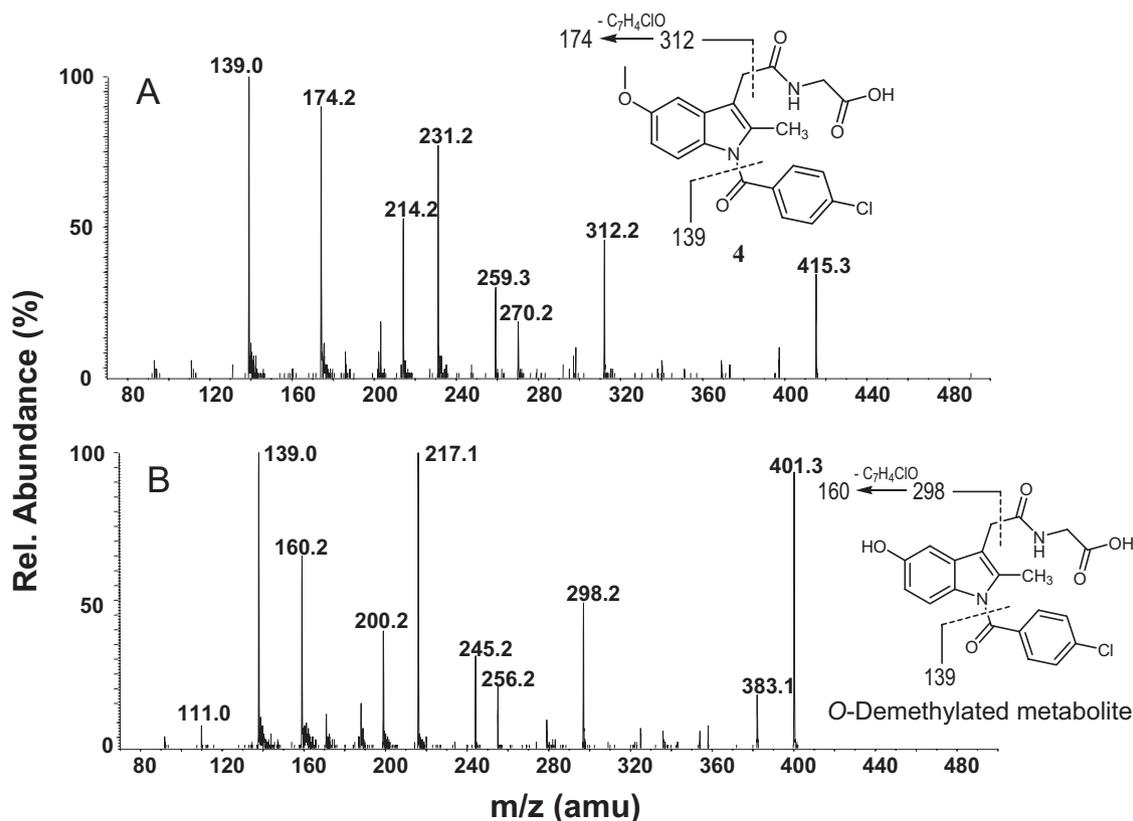
FIG. 8. CID spectrum of indomethacin-glycine amide (**4**) (A) and its *O*-demethylated metabolite (B). amu, atomic mass units.

its neutral amide derivatives (final concentration = 1 μM) was assessed by monitoring substrate consumption after incubation with human and rat liver microsomes in the presence of NADPH cofactor for 30 min at 37°C (Table 1). Also shown in Table 1 are the physio-

chemical parameters (molecular weight and logP) and the unbound fractions of the test compounds in rat plasma and rat liver microsomes that were predicted using the in silico methodology described previously (Gao et al., 2008). Consistent with previous results (Remmel et

TABLE 1

Rat and human liver microsomal stability of indomethacin and its amide derivatives 1 to 4

indomethacin: R = OH

amide 1: R = [structure]

amide 2: R = [structure]

amide 3: R = [structure]

amide 4: R = [structure]
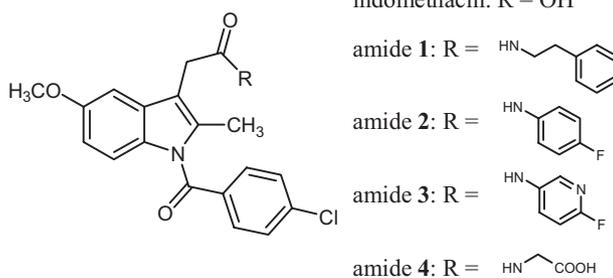
Compound	MW/LogP[a]	Rat Plasma/Microsomes Fraction Unbound[b]	$t_{1/2}$ (min)	
			Rat	Human
			min	
Indomethacin	357/4.18	0.030/0.91[c]	>90	>90
Amide 1	460/5.50	0.0045/0.13	1.0	1.5
Amide 2	450/5.85	0.0040/0.05	8.5	25
Amide 3	451/5.05	0.0070/0.14	8.0	23
Amide 4	414/3.54	0.030/0.93	>90	>90

MW, molecular weight.
[a] LogP values were calculated using ACD software (Advanced Chemical Development, Inc.).
[b] Fraction unbound estimates in rat plasma and rat liver microsomes were obtained using in silico models developed at Pfizer as described previously with human liver microsomes (Gao et al., 2008). Literature free fraction of indomethacin in rat plasma is 0.040 (Dawidowicz et al., 2008), indicating high confidence in the in silico predictions.

al., 2004), indomethacin-*N*-phenethyl amide (**1**) was highly unstable ($t_{1/2} \leq 2$ min) in rat and human liver microsomes supplemented with NADPH, whereas amides **2** and **3** were relatively more stable as reflected by the longer $t_{1/2}$ values. Unbound fraction estimates in rat microsomes and plasma were comparable for the three neutral amides. In contrast, the glycine amide derivative **4** was devoid of metabolic turnover in both rat and human liver microsomes ($t_{1/2} > 90$ min). Under these experimental conditions, parent NSAID indomethacin was resistant to metabolic turnover ($t_{1/2} > 90$ min). Consistent with lower logP values, the fractions unbound for indomethacin and glycine amide derivative **4** in rat microsomes and plasma were higher than those predicted for the more lipophilic neutral amides **1** to **3**. Indomethacin amides **1**, **2**, and **3** were stable ($t_{1/2} > 90$ min) in incubations lacking NADPH or liver microsomes from rat and human. Substrate depletion experiments in human liver microsomes were also induced in the presence of the P450 3A4- and P450 2D6-selective inhibitors ketoconazole and quinidine, respectively. As shown in Table 2, coincubation with ketoconazole rendered amides **1**, **2**, and **3** to be completely stable toward oxidation. Inclusion of quinidine had a less pronounced effect on metabolic turnover of indomethacin amide derivatives. Although the P450 phenotyping using isozyme-specific inhibitors could not be conducted for **4** because of lack of substrate depletion in microsomes, separate studies using recombinant P450 3A4, 2D6, and 2C9 isozymes revealed that only P450 2C9 was capable of *O*-demethylating **4** (data not shown).

In Vivo Pharmacokinetics. To evaluate whether the increased metabolic resistance of amides **2**, **3**, and **4** (compared with **1**) translates into improvements in clearance and oral bioavailability, we decided to examine the pharmacokinetics of amides **1** to **4** after intravenous and oral administration to Sprague-Dawley rats at 1 and 5 mg/kg, respectively. Table 3 summarizes the values (mean ± S.D.) of the pharmacokinetic parameters for **1**, **2**, **3**, and **4** after intravenous and oral administration. Plasma concentrations after intravenous administration of indomethacin-*N*-phenethyl amide (**1**) declined very rapidly resulting in an estimated CL_p value of 155 ± 41.5 ml/min/kg, which exceeded rat hepatic blood flow (70 ml/min/kg). In contrast, amide derivatives **2**, **3**, and **4** demonstrated significant attenuation in

TABLE 2

P450 isozymes responsible for metabolic turnover of indomethacin amides 1 to 3 in human liver microsomes

Indomethacin amide **4** was not tested because it was resistant to metabolic turnover.

Compound	% Inhibition of Substrate Depletion	
	Microsomes + Ketoconazole	Microsomes + Quinidine
Amide 1	96	<5
Amide 2	100	35
Amide 3	100	28

CL_p values. After oral administration of **1**, systemic exposure at all sampling points was below the limit of detection (5 ng/ml). In contrast, oral dosing of amides **2**, **3**, and **4** led to measurable systemic exposure, which allowed estimation of the corresponding C_{max} and $AUC_{0-\infty}$ values. The oral bioavailabilities of amides **2**, **3**, and **4** in the rat were 20, 38.5, and 37.6%, respectively.

Discussion

Rather than using MetaSite to predict metabolism for a large number of structurally diverse substrates, our objective here was a focused analysis of a small subset of compounds within a given chemical series for the purposes of lead optimization. Comparison of the predictions for indomethacin and **1** with published experimental data showed a high degree of accuracy (>80% success rate), which is in good agreement with published prediction rates of MetaSite for a large number of heterogeneous substrates (Cruciani et al., 2005; Zhou et al., 2006; Caron et al., 2007). Encouraged by these preliminary observations, we decided to test the accuracy of metabolite predictions for additional indomethacin amide derivatives for which no prior experimental knowledge on their metabolism was available. The overarching objective of this exercise was to evaluate whether the tool can be used in drug discovery to build metabolic resistance into metabolically labile compounds, a feature that could potentially translate into improvements into pharmacokinetic properties.

Given the knowledge that the metabolic instability of **1** was primarily derived from metabolism on the pendant phenethyl group, we

TABLE 3

Pharmacokinetic parameters of indomethacin-amides 1 to 4 in male Sprague-Dawley rats

Compounds were administered via intravenous bolus to fasted male Sprague-Dawley rats ($n = 3$) in 95% glycerol formal containing 5% DMSO. For oral studies, compounds were administered via gavage to fasted male Sprague-Dawley rats ($n = 3$) as a suspension in 0.5% methyl cellulose.

Compound	Dose	Route	C_{max}	T_{max}	CL_p	V_{dss}	$AUC_{0-\infty}$	$T_{1/2}$	F
	mg/kg		ng/ml	h	ml/min/kg	l/kg	ng · h/ml	h	%
Amide **1**	1.0	i.v.			155 ± 41.5	5.3 ± 1.2	114 ± 35.0	0.6 ± 0.1	
	5.0	p.o.	N.C.	N.C.			N.C.		N.C.
Amide **2**	1.0	i.v.			26.0 ± 9.40	2.3 ± 1.1	699 ± 240	1.1 ± 0.3	
	5.0	p.o.[a]	57.0	3.0			677		20
Amide **3**	1.0	i.v.			39.2 ± 4.50	2.0 ± 0.4	430 ± 49.0	1.0 ± 0.3	
	5.0	p.o.	120 ± 55.8	1.2 ± 0.7			828 ± 490		38.5
Amide **4**	1.0	i.v.			31.0 ± 7.00	0.7 ± 0.2	562 ± 150	1.4 ± 0.4	
	5.0	p.o.	154 ± 42.1	1.0 ± 0.8			1060 ± 167		37.6
Indomethacin[b]	1.0	i.v.			0.51 ± 0.04	0.19 ± 0.03		4.6 ± 1.0	

N.C., not calculated [systemic exposure below the lower limit of quantitation (5 ng/ml)].
[a] $n = 2$ rats.
[b] Intravenous pharmacokinetic data from Paine et al. (2008).

selected virtual indomethacin analogs **2**, **3**, and **4**, in which we resorted to introducing electron-deficient or polar amide substituents as standard tactics used in medicinal chemistry to build metabolic resistance around soft spots. For anilide analogs **2** and **3**, the electron-deficient fluorophenyl and fluoropyridinyl ring systems were deliberately chosen to avoid the potential for acetaminophen-type bioactivation to electrophilic quinone-imine intermediates. When the structures were presented to MetaSite, the software predicted a metabolic shift and assigned *O*-demethylation as the highest priority site for oxidation, a prediction that was fairly accurate as determined from experimental metabolite identification studies on these analogs. It is noteworthy to point out that the predictions were restricted to metabolism by certain P450 isozymes (P450 3A4 and 2D6 for the neutral amides **1**, **2**, and **3** and P450 2C9 specifically included for indomethacin and the glycine amide **4**) based on our input into the software. This input was primarily based on the experimental observations that P450 isozymes 2C9 and 3A4/2D6 are involved in the metabolism of indomethacin and its phenethyl amide derivative **1**. On the basis of this metabolism we inferred (and later confirmed) that P450 3A4/2D6 would also play a key role in the metabolism of neutral amides **2** and **3**. Because glycine amide **4** possessed a carboxylic acid group, we inferred (and later confirmed) that P450 2C9 would play an exclusive role in the metabolism of this anionic compound as per the norm with many P450 2C9 substrates (Lewis et al., 2002). In addition, it is of interest to note that MetaSite predictions are not quantitative in nature. Based on chemical reactivity, the software assigns hierarchy (major versus minor) to likely sites of metabolism but does not provide insights into the overall metabolic stability of the molecule as it relates to in vitro $t_{1/2}$ values and ultimately in vivo clearance. Evaluation of these latter attributes requires additional experimentation as was the case in our investigations wherein rat and human liver microsomal stability and rat pharmacokinetic data on amides **2**, **3**, and **4** had to be generated. Compared with **1**, neutral amides **2** and **3** were relatively more stable in NADPH-supplemented rat and human liver microsomes. In contrast, indomethacin and the glycine amide **4**, which contained free carboxylic acid substituents, were completely resistant to metabolism in liver microsomes from both species. Considering that microsomal unbound fractions of amides **1**, **2**, and **3** predicted from in silico computational models (Gao et al., 2008) were comparable (Table 1), the free intrinsic clearance values (amide **1**: 6646 ml/min/kg; amide **2**: 2034 ml/min/kg; and amide **3**: 772 ml/min/kg) obtained from scale-up of half-life data (normalized for nonspecific microsomal binding) (Obach, 1999), suggested that the strategy of attenuating metabolism via structural modification of the amide substituent in **1** had worked in our favor. Of much interest in this endeavor were the observations on the similarity in metabolic stability and free microsomal fraction of indomethacin and glycine amide **4** that resulted in comparable intrinsic clearance predictions of <10 ml/min/kg. The higher free fractions of indomethacin and glycine amide **4** in microsomes and plasma relative to the neutral amides **1** to **3** were anticipated, given their lower lipophilicity values.

As the next step in our exercise, we were interested in seeing whether the decreases in free intrinsic clearance value half-lives of amides **2** to **4** in liver microsomes translated into a lower clearance and greater oral bioavailability in the rat. In contrast with the hepatic blood flow limited clearance observed with **1**, neutral indomethacin amides **2** and **3** revealed moderate clearances in the range of 26 to 39 ml/min/kg. The possibility that higher plasma protein binding of amides **2** and **3** (compared with **1**) played a role in the diminished clearance can be ruled out given that the predicted unbound fraction of the neutral compounds in rat plasma is comparable (Table 1). Assuming that hepatic oxidative metabolism by P450 plays a major role in elimination, the clearance values for **2** and **3** will translate into hepatic extraction ratios of 0.37 to 0.55 (based on a rat hepatic blood flow of 70 ml/min/kg), respectively, and could result in maximum possible oral bioavailability ranging from 45 to 63%. The observed lower oral bioavailabilities for **2** ($F = 20\%$) and **3** ($F = 38.5\%$) suggest that solubility and/or gut extraction could play a role in limiting oral absorption for these compounds in the rat. The observed in vivo clearance and oral bioavailability of the glycinyl amide **4** was comparable with that estimated for the fluorophenyl and fluoropyridinyl amide derivatives **2** and **3**, respectively, despite free intrinsic clearance and plasma protein binding values comparable with that for the parent NSAID indomethacin. Although the in vitro-in vivo disconnect into **4** was not tested directly, plausible reason(s) are the existence of non-P450 clearance mechanism(s) such as phase II acyl glucuronidation and/or nonmetabolic elimination pathway such as organic anion transporter-mediated renal excretion in a manner similar to that discerned with indomethacin and most other carboxylic acid-containing NSAIDs (Apiwattanakul et al., 1999; Kouzuki et al., 2000; Sabolovic et al., 2000). With respect to the higher in vivo clearance compared with indomethacin, it is possible that **4** possesses a significantly greater affinity for glucuronidation enzymes and/or organic anion transporters than the parent NSAID.

Often, chemical intervention strategies to optimize metabolic stability via modulation of physiochemical properties or soft spot blocking tactics can have an adverse effect on primary pharmacology, resulting in loss of potency against a biological target or a shift in isozyme/receptor subtype selectivity. In the present investigation, this phenomenon becomes evident with the glycinyl amide derivative **4**.

Unlike the phenethyl amide derivative **1**, compound **4** is stable to degradation in rat and human microsomes, indicative of a significant improvement in metabolic stability. However, this advantage is offset by the fact that unlike **1**, **4** is not a selective COX-2 inhibitor; in fact the compound does not inhibit the activities of either COX enzymes (IC_{50} >10 μM) (Bartolini et al., 2007). In contrast, the neutral 4-fluorophenyl amide derivative of indomethacin **2** has been reported to maintain the potent and selective COX-2 inhibitory attributes of **1** [phenethyl amide (**1**): COX-2 IC_{50} 0.066 μM, COX-1 IC_{50} >66 μM; 4-fluorophenyl amide (**2**): COX-2 IC_{50} 0.066 μM; COX-1 IC_{50} >66 μM] (Kalgutkar et al., 2000b). Likewise, a close-in analog of the 4-fluoropyridinyl amide derivative **3**, in which the fluorine is replaced with a chlorine atom has been synthesized and shown to retain COX-2 potency and selectivity discerned with **1** (Kalgutkar et al., 2000b), suggesting that **3** would possess similar characteristics. Taken together, amides **2** and **3** represent a significant advantage over **1** in that they retain the primary pharmacology of **1** while offering a pharmacokinetic benefit due to improved metabolic stability.

In conclusion, MetaSite has not been designed to predict rates of oxidation (V_{max} and K_m) or to provide quantitative predictions, and furthermore its use is restricted to the major human P450 isozymes and their oxidative capacity. Nevertheless, as demonstrated in previous studies and in this work, the MetaSite methodology is automated and rapid and has relatively accurate predictions; consequently, it can be used as a metabolic site prediction tool at the early drug discovery stage in terms of both speed and accuracy. However, it is best to confirm the predictions with experimental data for a few compounds within a chemical series to ensure preciseness of the predictions. In addition, it is noteworthy to point out that the problem explored in our study was of relatively low complexity considering that the lead compounds possessed few metabolic soft spots. Consequently, the accuracy of MetaSite in predicting metabolism of complex molecules (with numerous options for metabolism) needs to be examined further. Finally, during the course of this investigation, we also realized that the integration of MetaSite predictions and experimental data, interpretation of the similarities and differences in metabolism, a priori knowledge on the P450 isozymes involved in metabolism, and other factors critically depend on the human expert.

References

Ahlström MM, Ridderström M, Zamora I, and Luthman K (2007) CYP2C9 structure-metabolism relationships: optimizing the metabolic stability of COX-2 inhibitors. *J Med Chem* **50:**4444–4452.

Apiwattanakul N, Sekine T, Chairoungdua A, Kanai Y, Nakajima N, Sophasan S, and Endou H (1999) Transport properties of nonsteroidal anti-inflammatory drugs by organic anion transporter 1 expressed in *Xenopus laevis* oocytes. *Mol Pharmacol* **55:**847–854.

Bartolini W, Cali BM, Chen B, Chien YT, Currie MG, Milne GT, Pearson JP, Talley JJ, Yang JJ, Zimmerman C, et al. (2007) inventors; Microbia Inc., Bartolini W, Cali BM, Chen B, Chien YT, Currie MG, Milne GT, Pearson JP, Talley JJ, Yang JJ, Zimmerman C, et al., assignees. Useful indole compounds. World patent WO2007070892 (A2). 2007 June 21.

Caron G, Ermondi G, and Testa B (2007) Predicting the oxidative metabolism of statins: an application of the *MetaSite*® algorithm. *Pharm Res* **24:**480–501.

Cruciani G, Carosati E, De Boeck B, Ethirajulu K, Mackie C, Howe T, and Vianello R (2005) MetaSite: understanding metabolism in human cytochromes from the perspective of the chemist. *J Med Chem* **48:**6970–6979.

Dahlin DC, Miwa GT, Lu AY, and Nelson SD (1984) *N*-Acetyl-*p*-benzoquinone imine: a cytochrome P-450-mediated oxidation product of acetaminophen. *Proc Natl Acad Sci U S A* **81:**1327–1331.

Dawidowicz AL, Kobielski M, and Pieniadz J (2008) Anomalous relationship between free drug fraction and its total concentration in drug-protein systems II. Binding of different ligands to plasma proteins. *Eur J Pharm Sci* **35:**136–141.

Gao H, Yao L, Mathieu HW, Zhang Y, Maurer TS, Troutman MD, Scott DO, Ruggeri RB, and Lin J (2008) In silico modeling of nonspecific binding to human liver microsomes. *Drug Metab Dispos* **36:**2130–2135.

Kalgutkar AS, Crews BC, Rowlinson SW, Marnett AB, Kozak KR, Remmel RP, and Marnett LJ (2000a) Biochemically based design of cyclooxygenase-2 (COX-2) inhibitors: facile conversion of nonsteroidal antiinflammatory drugs to potent and highly selective COX-2 inhibitors. *Proc Natl Acad Sci U S A* **97:**925–930.

Kalgutkar AS, Marnett AB, Crews BC, Remmel RP, and Marnett LJ (2000b) Ester and amide derivatives of the nonsteroidal antiinflammatory drug, indomethacin, as selective cyclooxygenase-2 inhibitors. *J Med Chem* **43:**2860–2870.

Kouzuki H, Suzuki H, and Sugiyama Y (2000) Pharmacokinetic study of the hepatobiliary transport of indomethacin. *Pharm Res* **17:**432–438.

Lewis DF, Modi S, and Dickins M (2002) Structure-activity relationship for human cytochrome P450 substrates and inhibitors. *Drug Metab Rev* **34:**69–82.

Nakajima M, Inoue T, Shimada N, Tokudome S, Yamamoto T, and Kuroiwa Y (1998) Cytochrome P450 2C9 catalyzes indomethacin *O*-demethylation in human liver microsomes. *Drug Metab Dispos* **26:**261–266.

Obach RS (1999) Prediction of human clearance of twenty-nine drugs from hepatic microsomal intrinsic clearance data: an examination of in vitro half-life approach and nonspecific binding to microsomes. *Drug Metab Dispos* **27:**1350–1359.

Obach RS, Kalgutkar AS, Soglia JR, and Zhao SX (2008) Can in vitro metabolism-dependent covalent binding data in liver microsomes distinguish hepatotoxic from nonhepatotoxic drugs? An analysis of 18 drugs with consideration of intrinsic clearance and daily dose. *Chem Res Toxicol* **21:**1814–1822.

Paine SW, Parker AJ, Gardiner P, Webborn PJ, and Riley RJ (2008) Prediction of the pharmacokinetics of atorvastatin, cerivastatin and indomethacin using kinetic models applied to isolated rat hepatocytes. *Drug Metab Dispos* **36:**1365–1374.

Remmel RP, Crews BC, Kozak KR, Kalgutkar AS, Marnett LJ, and Algutkar AS (2004) Studies on the metabolism of the novel, selective cyclooxygenase-2 inhibitor indomethacin phenethylamide in rat, mouse, and human liver microsomes: identification of active metabolites. *Drug Metab Dispos* **32:**113–122.

Sabolovic N, Magdalou J, Netter P, and Abid A (2000) Nonsteroidal anti-inflammatory drugs and phenols glucuronidation in Caco-2 cells: identification of the UDP-glucuronosyltransferases UGT1A6, 1A3 and 2B7. *Life Sci* **67:**185–196.

Zamora I, Afzelius L, and Cruciani G (2003) Predicting drug metabolism: a site of metabolism prediction tool applied to the cytochrome P450 2C9. *J Med Chem* **46:**2313–2324.

Zhou D, Afzelius L, Grimm SW, Andersson TB, Zauhar RJ, and Zamora I (2006) Comparison of methods for the prediction of the metabolic sites for CYP3A4-mediated metabolic reactions. *Drug Metab Dispos* **34:**976–983.

Address correspondence to: Dr. Amit S. Kalgutkar, Pharmacokinetics, Dynamics, and Metabolism Department, Pfizer Global Research and Development, Groton, CT 06340. E-mail: amit.kalgutkar@pfizer.com